Indian Journal of Pure & Applied Physics
Vol. 60, August 2022, pp. 634-643
DOI: 10.56042/ijpap.v60i8.63817

Suppression of Four Wave Mixing Effects Under Different Spectrally Efficient Modulation Techniques in Hybrid DWDM-OTDM Systems

Parashuram & Chakresh Kumar*

University School of Information, Communication & Technology,
Guru Gobind Singh Indraprastha University, New Delhi-110 078, India

Received 7 June 2022; accepted 18 July 2022

Next generation optical networks require high spectral efficiency to meet the demand of high bandwidth for ultra-long haul communication. Spectrally efficient modulations using hybrid DWDM-OTDM systems can be used to achieve this. However, fiber nonlinearities such as four-wave mixing (FWM) will increase simultaneously and this will degrade the performance of WDM optical system. This paper explores the FWM reduction in 32 channels, 40 Gb/s hybrid DWDM-OTDM network using RZ-OOK, 16-QAM and PDM-QPSK modulation format at 200 GHz and 100 GHz channel spacing. Optical received power, BER, Q- factor, eye diagram and FWM side band power are analyzed at -15dBm to +15dBm channel power. All these modulations have shown a significant reduction in FWM. In addition, the 16-QAM gives highest reduction in FWM along with least BER of 7.9×10^{-158} and maximum Q-value of 27.74.

Keywords: Four Wave Mixing (FWM); Group Velocity Dispersion (GVD); Channel spacing; QAM (Quadrature amplitude Modulation); PDM-QPSK; RZ-OOK; DWDM; Bit Error Rate (BER); Highly nonlinear fiber (HNLF) and OSNR

1 Introduction

Nowadays the communication system has become very advanced, along with that the way of using the internet has also changed. Because of this there is a need to continuously optimize the optical fiber communication to meet the demand of high-speed data rate and high bandwidth capacity. Dense Wavelength Division Multiplexing (DWDM) implementation filled this gap significantly[1-3]. In DWDM system, large numbers of channels are used to transmit the multiple data of many users simultaneously over a single fiber by decreasing channel spacing[4-6]. Reduction of channel spacing under a high data rate leads to nonlinearities in optical fiber communication. Some major nonlinearities such as cross phase modulation (XPM), self-phase modulation (SPM), four wave mixing (FWM), Stimulated Brillouin scattering (SBS) and stimulated Raman scattering (SRS) degrades the bandwidth efficiency and transmission distance in optical fiber system. FWM occurs due to variation in intensity dependent refractive index[7-9]. FWM is third order nonlinear Kerr effect which causes crosstalk in DWDM system due to generation of fourth signal after interaction of three co-propagating optical signals[10-12]. Kerr effect is the dependence of refractive index on the field. The newly generated frequency signal overlaps with the original frequency signals causing interchannel noise and power penalties, it can lead to data privacy issues. FWM has both merits and demerits. FWM demerits can be useful in wavelength conversion, parametric amplification pulse regeneration and switching[13-14].

FWM can be suppressed by techniques such as-introducing delay between channels, optical phase conjugation, decreasing input signal power, phase coherence between channels, fiber dispersion profile modulation and unequal input channel spacing[15-17]. Unequal channel spacing is not an optimum use of bandwidth. Both low dispersion and high input power are necessary for WDM system which leads to FWM that generates a new spectrum. Recently some approaches have been developed to mitigate the FWM using distinct advanced modulations and optical filters in DWDM systems[18-20]. Wu *et al.*[21] have studied optical crosstalk in a typical FBG–OC-based OXC and observed that the worst-case coherent crosstalk is about 22–26 dB higher than incoherent crosstalk, depending on the switching states of 2-2, OXCs and concluded that 2-2, OXC is efficient with

*Corresponding authors:
(Email: ckumardhan@gmail.com)

much improved intraband crosstalk to meet different requirements of practical systems. Which is followed by Sabat *et al*.[22], they have investigated a method for reducing the FWM effect using dual port dual drive Mach-Zehnder modulator and circular polarization (DPDDML) for a single mode fiber (SMF) of length 100 km, and bit rate of 10 Gbps with two channels having channel spacing of 0.5 nm. They have concluded that performance of the system has been improved as compared with the existing system (which uses Mach-Zehnder modulator) in terms of reducing the FWM effect in fiber optic communication system. An approach to reduce the FDM haven been investigated by Sajgalikova *et al*.[23]. Selvendran *et al*.[24] described an approach to mitigate FWM effect. Some approached to reduce nonlinearities have been developed using optical phase conjugation (OPC) and HOA in dense optical systems[25-27]. FWM effect have observed using different modulations schemes recently still these methods are not efficient and there is enormous scope to optimize nonlinearities. In this paper FWM reduction have been explored using spectrally efficient modulations in hybrid WDM-OTDMA network.

FWM is the phenomenon in which three photons are mixed to generate the fourth wave which may fall into the spectrum of one of the transmitted channels. This process obeys the conservation of momentum and energy which leads to the condition of phase matching. The fourth optical frequency is expressed as $\omega_{abc} = \omega_a + \omega_b - \omega_c$, where ω_a, ω_b and ω_c are frequencies of copropagating light waves inside the fiber. Generally, a WDM system generates $\frac{N^2(N-1)}{2}$ FWM signals (possible mixing products), where N are the transmitted signals. Moreover, Phase matching condition is represented by following equation (1)

$$\triangle k = \beta_d + \beta_c - \beta_a - \beta_b = (n_4\omega_d + n_3\omega_c - n_2\omega_b - n_1\omega_a)/c \quad \ldots (1)$$

where $\triangle k$ is the phase mismatching parameter and β_a, β_b, β_c and β_d are propagation constant. The FWM efficiency η_{FWM} depends on the channel spacing and significantly higher in dispersion shifted fiber (DSF) compare to standard fibers due to reduced value of dispersion. The propagation of a light wave pulse along z-axis can be expressed using nonlinear Schrodinger wave equation (NLSE) as following equation (2),

$$\frac{\partial U}{\partial z} = \beta_1 \frac{\partial U}{\partial t} + \frac{i}{2}\beta_2 \frac{\partial^2 U}{\partial t^2} - \frac{1}{6}\beta_3 \frac{\partial^3 U}{\partial t^3} = i\gamma|U|^2 U \quad \ldots (2)$$

Where U is normalized pulse amplitude, β_1 is lightwave group delay, β_2 is first order group velocity dispersion (GVD), β_3 is second order GVD, γ is nonlinearity coefficient ($\gamma = \frac{\omega n_2}{cA_{eff}}$), n_2 is Kerr coefficient (this is refractive index nonlinear coefficient) and A_{eff} is effective core area.

If we considering that the three channels of frequencies ω_a, ω_b and ω_c are copropagating inside the fiber and also considering that they are not suppressed by mixing products then the time varying averaged optical power for fourth produced frequency component ω_{abc} can be expressed using equation (3)

$$P_{FWM}(l) = |U(l)|^2 = \eta_{FWM}\left(d_{FWM}\gamma l_{eff}\right)^2 P_a P_b P_c e^{-\alpha l} \quad \ldots (3)$$

where P_a, P_b *and* P_c are launched channel input powers, l_{eff} is fiber's effective length, α is the fiber attenuation coefficient, and d_{FWM} is the degeneracy factor of FWM. $d_{FWM} = 1$ when $a = b$ and $d_{FWM} = 2$ when $a \neq b$. The parameter η_{FWM} is FWM efficiency and is represented as the following equation (4) and (5)

$$\eta_{FWM} = \frac{1}{1+\left(\frac{\triangle k}{l}\right)^2}\left[1 + \frac{4e^{-\alpha l}\sin^2(\triangle k l/2)}{\left(1-e^{-\alpha l}\right)^2}\right] \quad \ldots (4)$$

and, $\triangle k = \frac{2\pi\lambda^2}{c}\Delta\nu_{ch}{}^2\left[D + \Delta\nu_{ch}\frac{\lambda^2}{c}\frac{dD}{d\lambda}\right]$ … (5)

where, $\Delta\nu_{ch}$ is channel spacing (nm), D is dispersion (ps/(nm-km)) at wavelength 1550 nm, $\triangle k$ is phase mismatch parameter, l is fiber length and λ is channel wavelength. For enabling spectrally efficient system, spectral efficiency should exceed 0.2 bit/sec/Hz. Some optimized techniques such as advanced modulation techniques between neighboring channels are required to meet this spectral efficiency. Spectral efficiency (η_{SE}) is expressed mathematically as equation (6),

$$\eta_{SE} = \frac{\sum_{i=1}^{n} r_{b,i}}{n\Delta\nu_{ch}} \quad \ldots (6)$$

where, n is number of channels in WDM system, $r_{b,i}$ is the bit rate of i^{th} channel (Gb/sec), η_{SE} is spectral efficiency in GHz , $\Delta\nu_{ch}$ is channel spacing in GHz and $\sum_{i=1}^{n} r_{b,i}$ is the total capacity (C).

In this paper, we demonstrated the suppression of FWM in 32 channels 40 Gb/s hybrid DWDM-OTDM system using the spectrally efficient advanced modulation techniques such as RZ-OOK signal generator, 16-QAM and PDM-QPSK. In DWDM transmission system nonlinearities can be reduced significantly using spectrally efficient modulation techniques.

Furthermore, this paper is organized as follows: section 1 introduced the FWM basics section 2 describes the hybrid DWDM-OTDM transmission system, advanced modulation and detection techniques. In section 3, simulation results are analyzed and effect of spectrally efficient modulation techniques in reducing the FWM in hybrid DWDM-OTDM network is observed and finally the conclusion is made in section 4.

2 System Design

The proposed 40 Gb/s hybrid system design DWDM-OTDM architecture is shown in the Fig. 1. It consists of semiconductor optical amplifiers (SOAs), advanced spectrally efficient modulators and dispersion compensated fibers (DCF). 32 distinct frequency channels with 100 GHz and 200 GHz channel spacing are considered for simulation, where each channel transmits 40Gbps of information. The SOA is used to compensate the losses along the fiber to maintain the sufficient signal power. CW lasers generate the optical signals and RZ-OOK signal generator, 16-QAM and PDM-QPSK modulators are used in transmitter followed by a hybrid DWDM multiplexer (HMUX) and corresponding hybrid demultiplexer (HDeMUX) over 60 km SMF-DCF high nonlinear fiber (HNLF) link. To demonstrate the FWM effects, simulation parameters of SOA gain amplifier and SMF-DCF are shown in Table 1 and Table 2 respectively. DCF is followed by SOA with zero noise figure. Optical power of laser sources is kept at -4dBm with optical linewidth of 10 MHz. Channel's central frequencies lie is in the range of 193 THz to 199.2THz with 200GHz channel spacing and 193 THz to 194.1 THz with 100 GHz channel spacing. DCF is used to compensate the dispersion occurred due to SMF. DCF has negative dispersion slope and dispersion to reduce the nonlinearity like FWM but it degrades signal quality for long haul communication.

2.1 Spectrally efficient modulators with their spectra

SOA is used as a power booster at the output of hybrid multiplexer shown in Fig. 1. The simulation setup of RZ-OOK signal generation incorporating cascaded MZM shown in Fig. 2(a) for 40 Gb/s data rates. The block diagram of RZ-OOK transmitter

Table 1 — Parameters of the SOA gain amplifier to analyze the FWM effects under different techniques.

Parameters	Value/Unit
Carrier density at transparency	$1.4x10^{24}/m^3$
Recombination Coefficient	$1.43x10^{8}/s$
Radiative recombination coefficient	$1x10^{-16}m^3/s$
Optical confinement factor	0.3
Injection Current	0.15A
Indirect Auger Coefficient	$10^{-30}cm^6s^{-1}$

Table 2 — Simulation parameters of SMF and DCF for demonstration of FWM effects.

Parameters	Fiber type	
	SMF	DCF
Fiber length (Km)	50	10
Attenuation (dB/Km)	0.2	0.5
Dispersion slope (ps/nm^2/Km)	0.075	-0.3
Dispersion (ps/nm/km)	16.75	-85
Effective Area (μm^2)	70	22
PMD coefficient	0.2	0.2
Differential group delay(ps/Km)	3	3

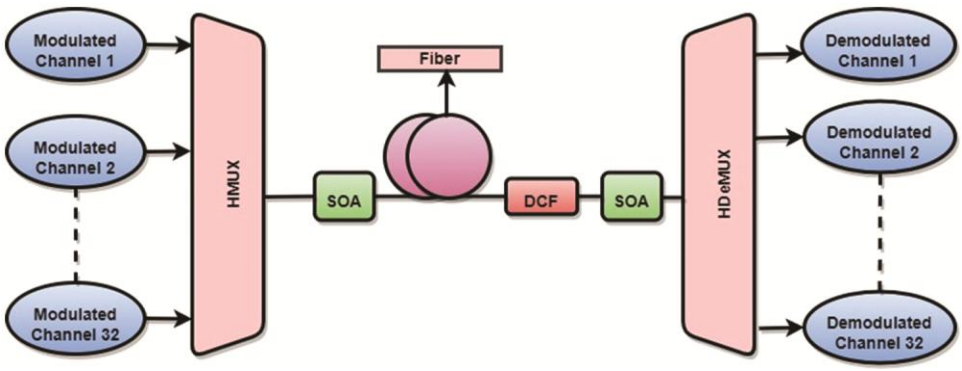

Fig. 1 — Schematic of the hybrid DWDM-OTDM architecture employing spectrally efficient higher order optical modulation

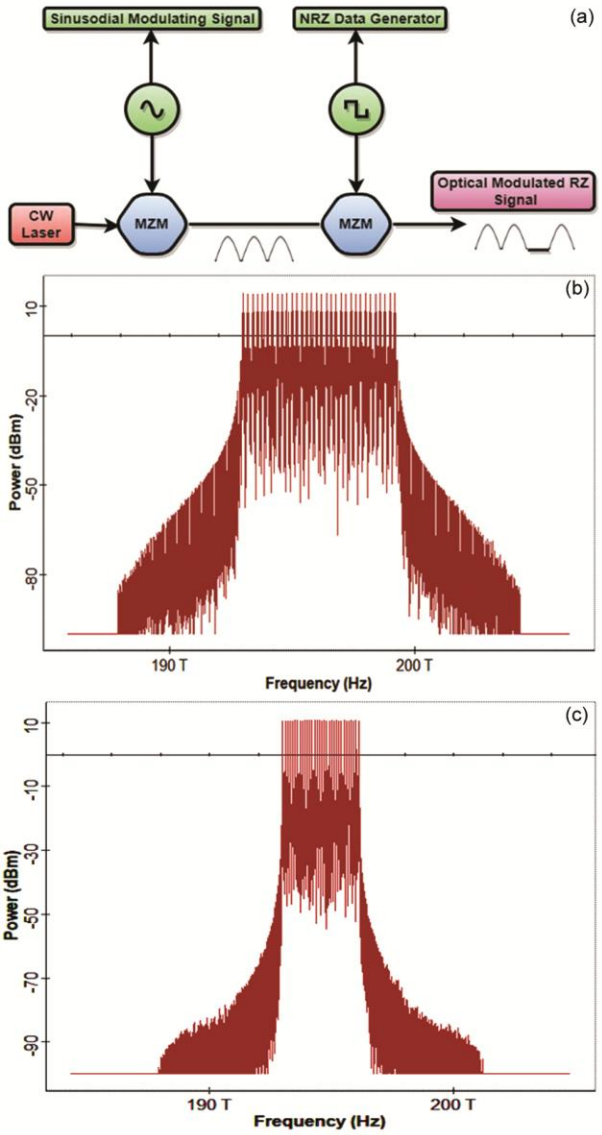

Fig. 2 — (a) RZ-OOK signal generation incorporating cascaded and its output spectrum power at (b)200 GHz channel spacing and (C) 100 GHz channel spacing

consists of a CW laser source followed by two cascaded connected Mach-Zehnder modulator (MZM). First MZM is used as pulse carver. Pseudorandom bit sequence (PSRB) of length $2^{31}-1$ and NRZ data generator used to drive the second MZM.

Figure 2(b,c) are shown the output spectrum of RZ-OOK modulation at 200 GHz and 100 GHz respectively. RZ-OOK modulation gives better spectral efficiency as its output spectrum is narrowed at central frequency. RZ-OOK modulation scheme is more efficient to polarization mode dispersion (PMD) and nonlinearity compare to NRZ-OOK. The input and output electric fields are related as, in equation (7),

$$E_o(t) = E_i(t)\, cos(\frac{\Delta\phi_{mzm}\,(t)}{2}) = E_i(t)\, cos(\frac{V(t)}{2V_\pi}\pi) \quad \ldots (7)$$

where $\Delta\phi_{mzm}\,(t)$ is phase difference induced between lower and upper arm. D.C biasing for operation of MZM is $-V_\pi/2$ and peak to peak modulation of driving voltage V_π so that π phase shift is generated on the photonic carrier. $V(t)$ is time dependent signal driving voltage (externally applied voltage). The power transfer function of MZM system is represented as, in equation (8),

$$P_{out}(t) = \alpha P_{in} \cos^2(\frac{v(t)}{V_\pi}\pi) \quad \ldots (8)$$

where transferred output power is $P_{out}\,(t)$ and input power from laser source is P_{in} and α is modulator's total insertion loss. Typical value of optical power loss within the modulator is max 5dB. Optical power loss is termed as insertion loss.

Furthermore, PDM-QPSK modulation scheme have been analyzed. The experimental setup of polarization division multiplexing-quadrature phase shift keying (PDM-QPSK) transmitter is shown in Fig. 3(a) for 40 Gb/s data rates. Fig. 3(b) and Fig. 3(c) shows the output spectrum of RZ-OOK modulation at 200 GHz and 100 GHz respectively. PDM-QPSK modulation gives better spectral efficiency as its output spectrum is more narrowed at central frequency compare to RZ-OOK modulation. I-Q modulator for single polarization or dual polarization is used to design PDM-QPSK and PDM-16QAM transmitter. For long haul communication PDM-QPSK is preferred while PDM-16QAM is preferable for metro application. PDM-QPSK is a hybrid modulation format. Polarization beam combiner (PBC) is used to combine the orthogonally modulated differently polarized signal. Polarization beam splitter (PBS) is used to split the optical beam generated from continuous wave laser source (CW laser) into X and Y polarized orthogonal states. Pseudorandom bit sequence generator (PSRB) is followed by serial to parallel converter (S/P). S/P is used to divide the data in different stream and further modulated over different polarization state using quadrature phase shift keying (QPSK) modulator.

In additional, another spectrally modulation scheme 16-QAM have been analyzed and proposed. The simulation setup of 16-QAM transmitter is shown in Fig. 4(a) for 40 Gb/s data rates. Fig. 4(b) and Fig. 4(c) shows the output spectrum of RZ-OOK modulation at

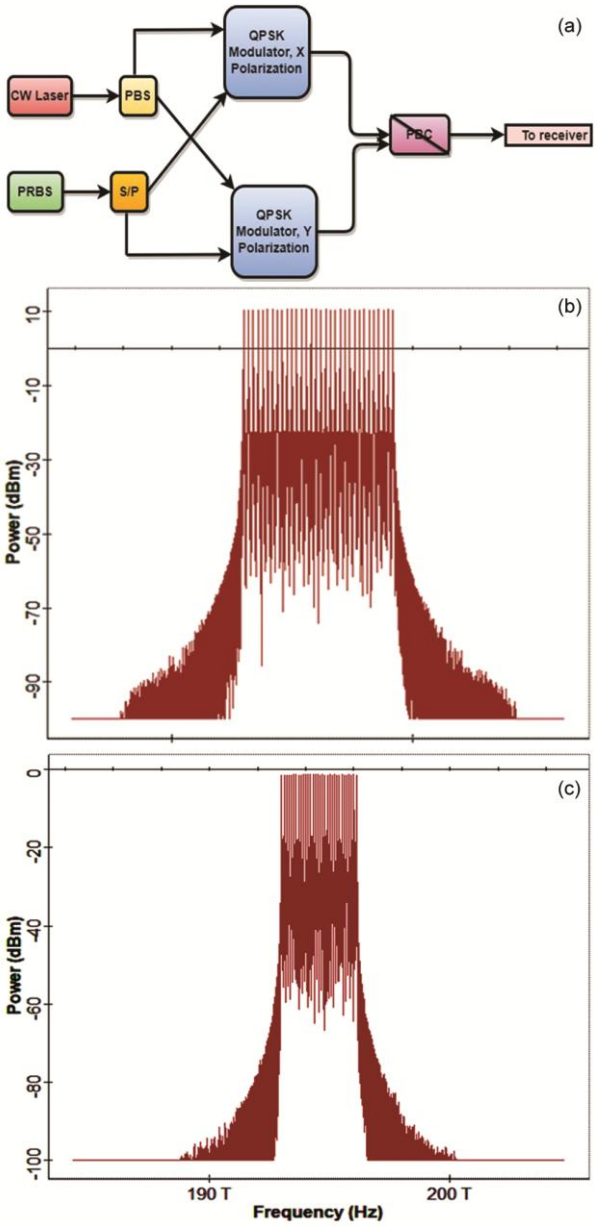

Fig. 3 — (a) PDM-QPSK Transmitter and its optical spectrum and its optical spectrum power at (b) 200 GHz channel spacing and (C) 100 GHz channel spacing

200 GHz and 100 GHz respectively. 16-QAM modulation provides optimum spectral efficiency as its output spectrum is maximally narrowed at central frequency among RZ-OOK, PDM-QPSK and 16-QAM. It consists of integrated I-Q modulator, 3dB attenuators, Mach-Zehnder modulator (MZM) and Phase modulator (PM). Each data stream of 40Gbps generated by PSRB is modulated by a 16-QAM modulator over a distinct polarized laser beam. The I and Q lights with 90° phase differences are multi-order intensity modulated by an IQ modulator (IQM).

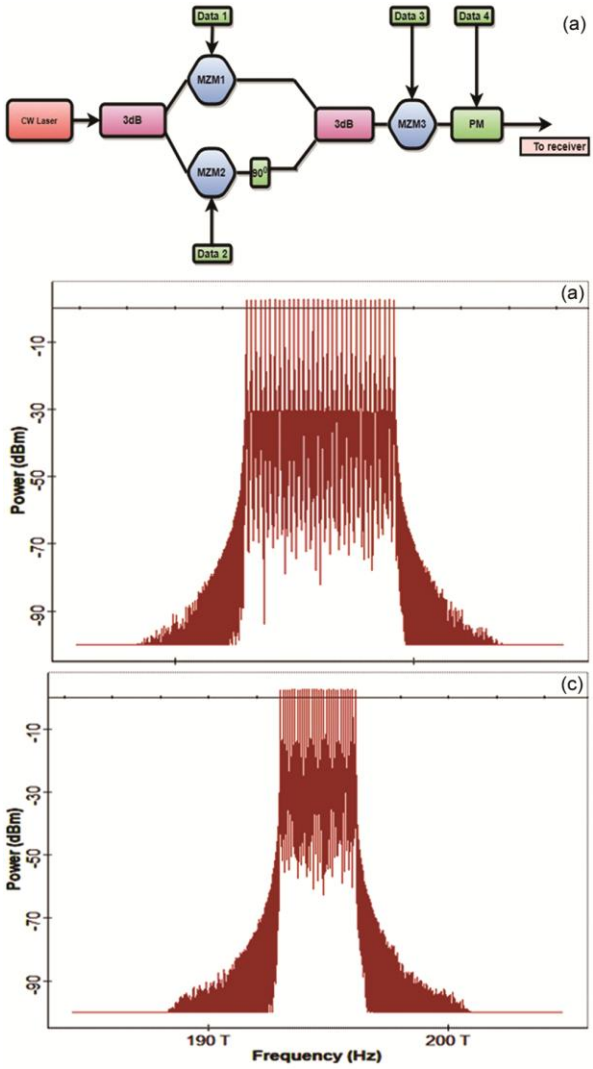

Fig. 4 — (a) 16-QAM transmitter and its optical spectrum power at (b)200 GHz channel spacing and (C) 100 GHz channel spacing.

Average energy for m-QAM constellation is $E_{avg}\,(QAM) = 2(1 - \frac{1}{m})$ where m is number of constellation points.

2.2 Receivers

At receiver side output of the hybrid demultiplexer (HDeMUX) is passed through the corresponding demodulator followed by filter for bit error test (BERT) measurement. BERT is used to analyze the signal quality. Low pass filter (LPF) is used to recover the signal reducing the noise. The set values for simulation are as follows- responsivity of pin detector is 1 A/W, LPF bandwidth is 1.2nm and dark current is 10nm. Fig. 5 shows simulation setup of RZ-OOK receiver. RZ-OOK receiver consists of a PIN photodiode followed by low pass filter.

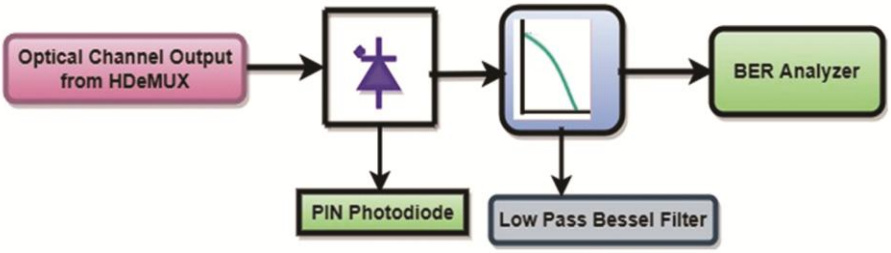

Fig. 5 — RZ-OOK Receiver.

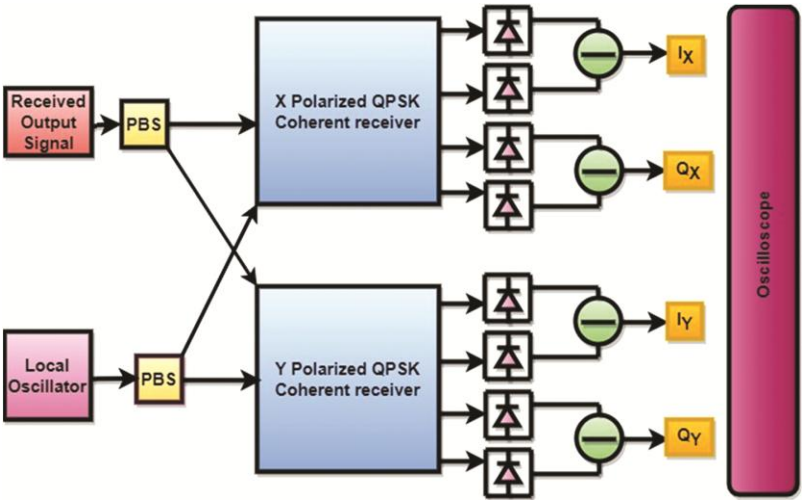

Fig. 6 — Polarization diversity coherent receiver.

Polarization diversity coherent receiver is shown in Fig. 6 for detection of PDM-QPSK and 16-QAM transmitted signal. Coherent detection of optical signal is processed in electrical domain. Complexity in terms of interferometric optical demodulation structure is decreased during phase to intensity modulation shift. Transmission impairments are compensated significantly using coherent detection. More tunable WDM receivers with high selective channel operations can be designed using PDM coherent detection. In coherent detection, optical signal light is first interacted with a local oscillator (LO) laser followed by 3dB coupler prior to photodetection. For spectrally efficient modulation at high data rates, homodyne coherent detection technique is more advantageous over heterodyne counterparts for future optical network. The frequencies of signal laser and local oscillator should be matched in homodyne receiver while a stable intermediate frequency (IF) at $\Delta\omega = \omega_s - \omega_{LO}$ is required in the heterodyne receiver when ω_s and ω_{LO} are frequencies of the signal and local oscillator light.

Each receiver unit uses a local oscillator (LO) laser and a polarization beam splitter (PBS) to detect the polarized information signal. The LO must be polarized at 45° with reference to PBS. Polarization of the signal and local oscillator affects the value of photocurrent. Photocurrents are combined electrically after photodetection. In-phase and quadrature signals of both frontends are added. The four photocurrents are converted from analog to digital then followed by digital equalization. The in-phase and quadrature phase electrical signals of the orthogonal polarization states are amplified with an electrical amplifier (EA) followed by LPF.

3 Results and Discussion

Distinct spectrally efficient modulated 32 channel hybrid DWDM-OTDM system is taken for simulation. Each channel has 40Gb/s data rates. Center frequencies are varying from 193 THz to 199.2 THz for 200 GHz channel spacing and 193 THz to 194.1 THz for 100 GHz channel spacing. The simulation parameters of SOA, SMF & DCF are shown in Table 1 and Table 2. The input power of laser is varying from -15dBm to 15dBm to analyze the FWM effect for DWDM system using RZ-OOK, PDM-QPSK and 16-QAM modulation schemes.

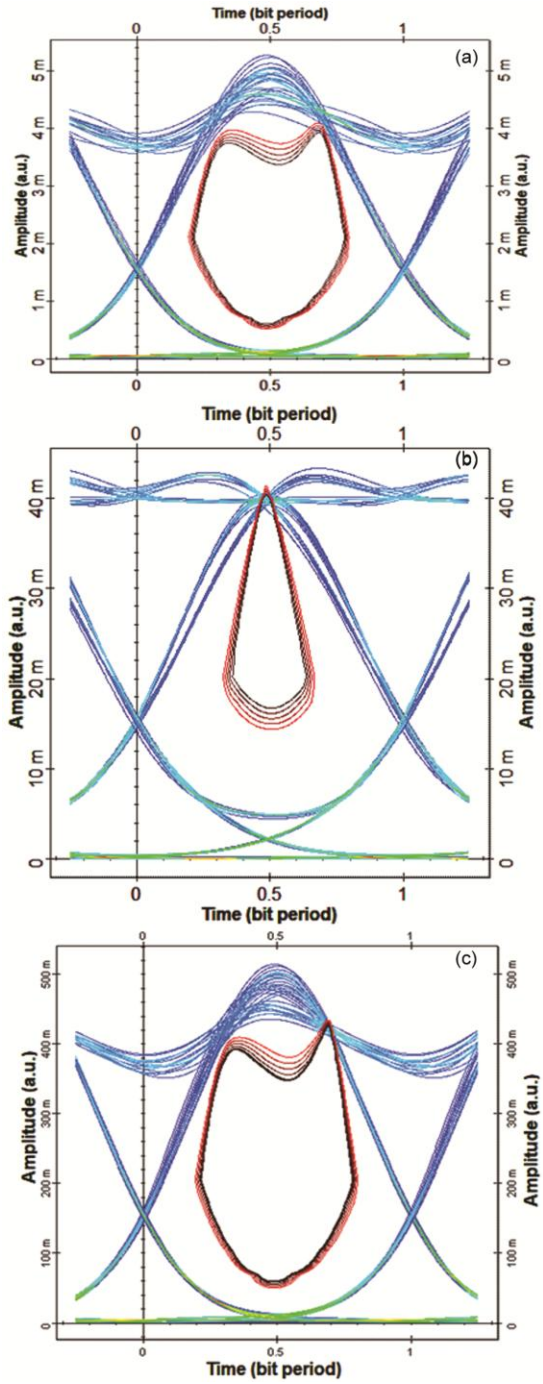

Fig. 7 — Eye diagram at 200 GHz channel spacing for (a) RZ-OOK, (b) PDM-QPSK and (c) 16-QAM modulation schemes.

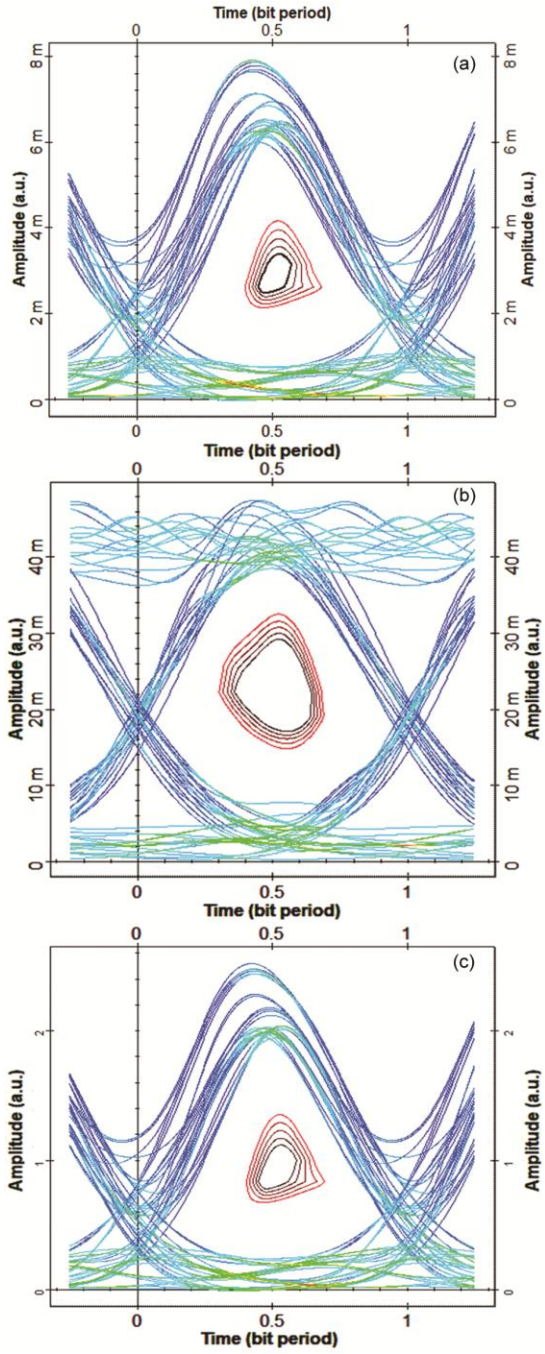

Fig. 8 — Eye diagram at 100 GHz channel spacing for (a) RZ-OOK, (b) PDM-QPSK and (c) 16-QAM modulation schemes.

Fig. 7 and Fig. 8 display the eye diagram for different modulation schemes at 200 GHz channel spacing and 100GHz channel spacing respectively. Eye heights are 0.00392276 a. u., 0.00268865 a. u. and 1.26273 a. u. at 100 GHz frequency spacing for RZ-OOK, PDM-QPSK and 16-QAM modulation schemes respectively. Moreover, for 200 GHz channel spacings, eye heights are 0.673828 a. u., 0.0314085 a. u. and 0.393191 a. u. for RZ-OOK, PDM-QPSK and 16-QAM modulations respectively.

Fig. 7 illustrates that eye diagram of 100GHz channel spacing has more impairments than 200 GHz channel spacing. Fig. 8 illustrates that 16-QAM provides a higher and better eye diagram. Eye diagram for 200 GHz channel spacing is clearer.

Q- values are 7.98, 11 and 13.79 for RZ-OOK, PDM-QPSK and 16-QAM modulation schemes at 100 GHz channel spacing. In additional, Q- values are 20.50, 22.50 and 27.74 for RZ-OOK, PDM-QPSK and 16-QAM modulation schemes at 200 GHz channel spacing

Figures 9 & 10 shows the relationship between the FWM power and the input power for different modulation format at 100 GHz and 200 GHz channel spacing. At 100 GHz frequency spacing, values of FWM power ranges from -79 dBm to -52 dBm in RZ-OOK, -85 dBm to -56 dBm in PDM-QPSK and -89 dBm to -60 dBm in 16-QAM at -15 dBm to +15 dBm channel power. Furthermore, At 200 GHz frequency spacing, values of FWM power ranges from -93 dBm to -65 dBm in RZ-OOK, -112 dBm to -86 dBm in PDM-QPSK and -114 dBm to -89 dBm in 16-QAM at -15 dBm to +15 dBm channel power. It is observed that FWM sideband power (crosstalk) is increasing with increase in launched signal power and decreasing with increase in channel spacing. FWM is dominating at lower power. It is observed that FWM sideband power (FWM crosstalk) is highest in RZ-OOK modulation and lowest in 16-QAM transmitter at different input power.

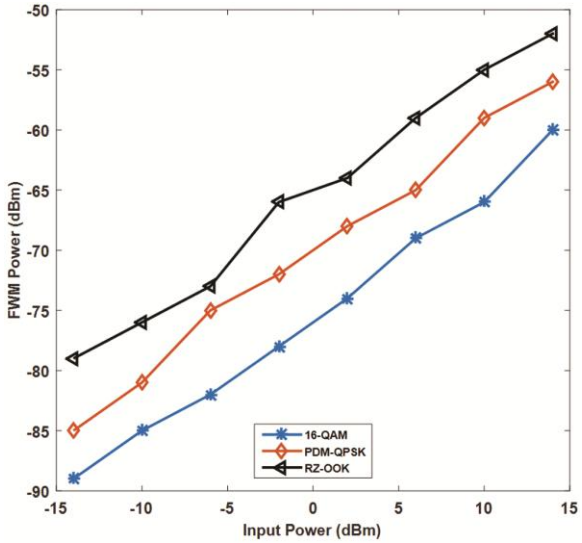

Fig. 9 — FWM power as a function of the input power for different modulation schemes at 100 GHz Channel spacing.

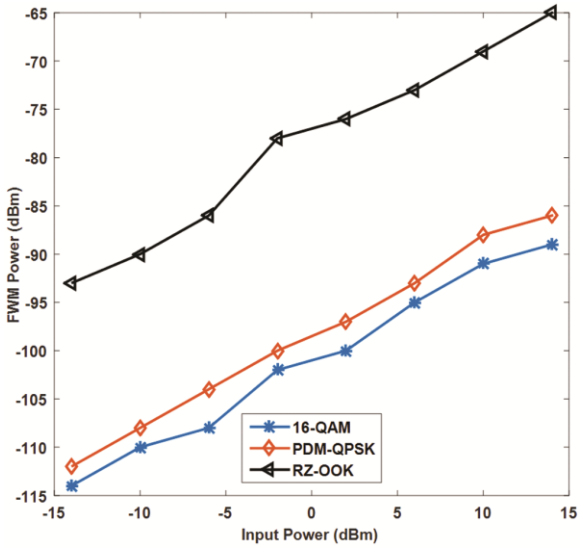

Fig. 10 — FWM power as a function of the input power for different modulation schemes at 200 GHz Channel spacing.

Fig. 11 and Fig. 12 displays the variation of bit error rate (BER) with received input power for

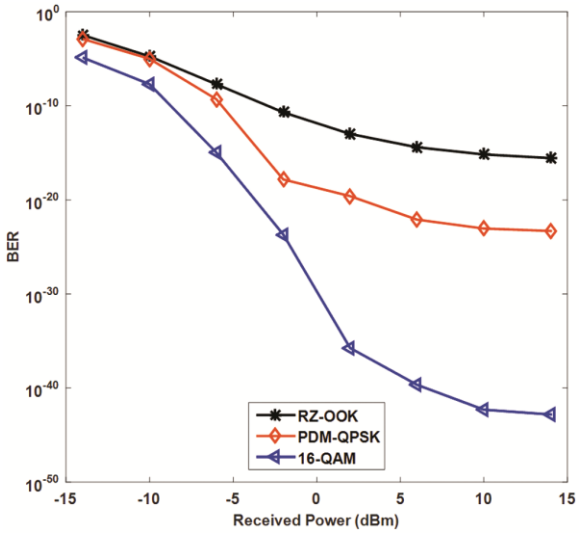

Fig. 11 — BER versus Received Power (dBm) at channel spacing 100GHz.

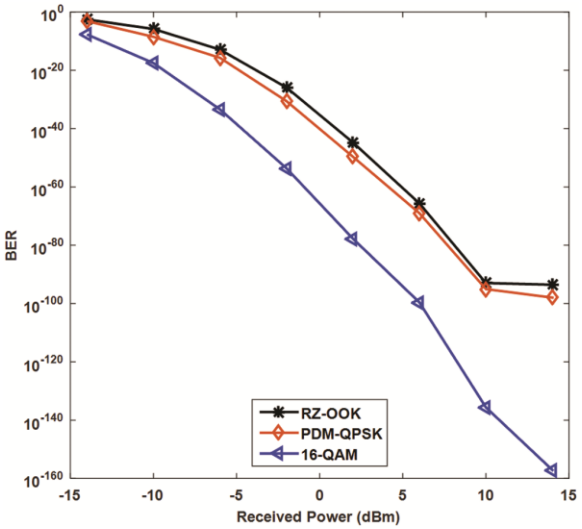

Fig. 12 — BER versus Received Power (dBm) at channel spacing 200GHz.

Table 3 — Results of the FWM effects under different modulation schemes at 100 GHz and 200 GHz frequency spacing.

Modulation Scheme	Channel spacing	FWM Power in dBm (Crosstalk)	FWM Reduction (dBm)	BER	Q
RZ-OOK	100 GHz	-55	-65	2.8×10^{-16}	7.98
PDM-QPSK	100 GHz	-70	-70	5×10^{-24}	11
16-QAM	100 GHz	-67	-76	1.51×10^{-43}	13.79
RZ-OOK	200 GHz	-66	-69	2.97×10^{-94}	20.50
PDM-QPSK	200 GHz	-88	-98	1.1×10^{-98}	22.50
16-QAM	200 GHz	-97	-101	7.9×10^{-158}	27.74

Table 4 — Comparison of present work with recent research works related to FWM suppression.

Parameter	N. Sharma et al. [18]	N. K. Sabat et al. [22]	Haider Jabber et al. [20]	S. Selvendran et al. [24]	H. U. et al. [19]	A. Chauhan et al. [25]	C. Kumar et al. [26]	G. Kumar et al. [27]	Present Work
Technology	Gaussian Generator, Raised Cosine Generator and Circular Polarizer	DPDDMZ and Circular Polarization	RZ-FSK, DPSK and Duobinary Modulation	NRZ, RZ-DQPSK, CSRZ-DPSK, D-RZ, and CSRZ	Gaussian Generator, Raised Cosine Generator and Duobinary Modulation	Ultra-Dense WDM, OPC	Super Dense O. C. using HOA	OPC	RZ-OOK, PDM-QPSK, 16-QAM Modulations in Hybrid DWDM-OTDMA Network.
No. of Channels	16	-	2	32	16	-	260	32	32
Channel Spacing	100 GHz	0.5 nm	0.4 nm	200 GHz	100 GHz	25 GHz	100GHz	0.4 nm	100 GHz, 200 GHz
Data Rate Per Channel	10Gbps	1 Gbps	40 Gbps	40 Gbps	10-20 Gbps	10 Gbps	10 Gbps	10 Gbps	40 Gbps
Maximum Q-Factor (Quality Factor)	18.3942	-	17.3	13.01	10	13.9	-	15 (at Km)	27.74
Minimum Bit Error Rate (BER)	-	-	4.56×10^{-68}	3.79×10^{-39}	-	-	4×10^{-5}	10^{-75}	7.9×10^{-158}
FWM Side Band Power (Crosstalk)	-81dBm	-100 dBm	-55 dBm	-45 d Bm	-82 dBm	-94.08 dBm	-50 dBm	80 dBm	-101 dBm
Channel Frequency	193.1-194.6 THz	1550 nm	1550 nm	192-198.2 THz	193.1-194.6 THz	193.07-193.16 THz	192.8-194 THz	1.53-1.565 μm	193-199.2 THz

different modulation schemes at 100 GHz channel spacing and 200 GHz channel spacing respectively. At 100 GHz frequency spacing, values of bit error rate (BER) ranges from 0.0033 to 2.8×10^{-16} in RZ-OOK, 0.0013 to 5×10^{-24} in PDM-QPSK and 1.35×10^{-5} to 1.51×10^{-43} in 16-QAM at -15 dBm to +15 dBm channel power. Furthermore, at 200 GHz frequency spacing, values of bit error rate (BER) ranges from 0.00285 to 2.97×10^{-94} in RZ-OOK, 0.00075 to 1.1×10^{-98} in PDM-QPSK and 2.01×10^{-8} to 7.9×10^{-158} in 16-QAM at -15 dBm to +15 dBm channel power.

It is observed from Fig. 11 and 12 that bit error rate improves as received power increases and degraded with reduction in channel spacing. BER is least in 16-QAM modulation and highest in RZ-OOK modulation at distinct received power. Table 3 summarizes all the simulation results and shows the suppression in FWM crosstalk using different modulation schemes for 200GHz and 100 GHz channel spacing in a 32 channel 40 Gb/s hybrid DWDM-OTDM network. Furthermore, Table 4 shows comparison of proposed work with recent research papers.

4 Conclusion

Spectrally efficient advanced modulations have been proposed to suppress the FWM effect over long haul hybrid DWDM-OTDM transmission system of 32 channels. Three different modulations have been proposed in hybrid DWDM-OTDM system. A comparative analysis is carried out at 100 GHz and 200 GHz channel spacing for RZ-OOK, PDM-QPSK and 16-QAM modulation schemes using the optisystem 7.0 simulator. BER, Q-value, received power, eye diagram and Optical spectrum have been analyzed for different modulation techniques. We have demonstrated the FWM power variation with

varying input power using different modulation schemes. It has been observed that 16-QAM modulation provides the highest reduction in FWM power along with least BER of 7.9×10^{-158} and maximum Q-value of 27.74 among all proposed modulation techniques. Analysis have been done for channel power -15 dBm to 15 dBm. RZ-OOK modulation provides least reduction in FWM and PDM-QPSK provides moderate reduction. Minimum BER of RZ-OOK, PDM-QPSK and 16-QAM modulation schemes are 2.97×10^{-94}, 1.1×10^{-98} and 7.9×10^{-158} respectively and correspondingly maximum Q- values are 20.5, 22.5 and 27.74 for 200GHz channel spacing. For 100GHz channel spacing, minimum BER of RZ-OOK, PDM-QPSK and 16-QAM modulation schemes are 2.8×10^{-16}, 5×10^{-24} and 1.51×10^{-43} respectively and correspondingly maximum Q- values are 7.98, 11 and 13.79. It is observed that suppression of FWM effect is highest in 16- QAM and least in RZ-OOK. Based on our analysis 16-QAM modulation is more efficient than other modulations. It is concluded that a trade-off has to be made between FWM reduction and data rates among different modulation techniques.

References

1 Boffi P, *et al*., *Opt Commun*, 237 (2004) 319.
2 Dahdah N E, Govan D S, Jamshidifar M, Doran N J & Marhic M E, *IEEE J Sel Top Quantum Electron*, 18 (2012) 950.
3 Sabapathi T & Sundaravadivelu S, *Opt Int J Light Electron Opt*, 122 (2011) 1457.
4 Mahad F D, Supa'at A S M, Idrus S M & Forsyth D, *Opt Int J Light Electron Opt*, 124 (2013) 1.
5 Lawan S H & Mohammad A B, *Opt Quantum Electron*, 50 (2018) 91.
6 Sharma V & Kaur R, Int J Comput Appl, 46 (2012) 10.
7 Kirti R & Kaur P, *J Eng Appl Sci*, 12 (2017) 5462.
8 Singh S, Singh S & Mohammadi Q M, *Opt Fiber Technol*, 52 (2019) 1.
9 Qin J, Liu C, Huang Z, Su S & Zhang Y, Optik, 136 (2017) 480.
10 Cho P S & Khurgin J B, *IEEE Photon Technol Lett*, 15 (2003) 162.
11 Noshada M & Rostamia A, *Opt Int J Light Electron Opt*, 123 (2012) 758.
12 Mehera R & Joshi A, *Int J Electron Electr Eng*, 7 (2014) 97.
13 Kaler R & Kaur G, *Optoelectron Adv Mater Rapid Commun*, 15 (2021) 49.
14 Kaur G & Aggarwal M, *Int J Adv Res Electr Electron Instrum Eng*, 6 (2017) 5131.
15 Singh N & Goel A K, *An Int J Eng Sci*, 17 (2016) 382.
16 Dhivya M, Rajini J H & Selvi S T, *IEEE-Int Conf Comput Signal Process (ICCP)*, (2016) 2180.
17 Agrawal G P, "Nonlinear Fiber Optics", Fourth edition, Academic Press, Chapter no. 10 (2001) 368.
18 Sharma N, Singh H & Singh P, Proceedings of the 5th *Int Conf Commun Electron Syst (ICCES)*, (2020) 343.
19 Manzoor H U, Manzoor T, Hussain A, Aly M H & Manzoor S, Transaction of Electrical Engineering, *Iran J Sci Technol*, (2019).
20 Abed H J, Din N M, Al-Mansoori M H, Abdullah F & Fadhil H A, *Ukr J Phys*, 58 (2013) 4.
21 Wu X, Lu X, Ghassemlooy Z & Wang Y, *IEEE Photon Technol Lett*, 14 (2002) 2.
22 Sabat N K, Rao B S & Patnaik B, *IEEE-ICACCI*, (2017) 1946.
23 Šajgalíková J, Litvik J & Dado M, *ELEKTRO*, Strbske Pleso, (2016) 92.
24 Selvendran S & Sivanantharaja A, *J Nonlinear Opt Phys Mater*, 22 (2013) 3.
25 Chauhan A, Vaish A & Verma A, *J Opt Commun*, (2018).
26 Kumar C & Kumar G, SN Applied Sciences, *Nature*, 2019.
27 Kumar G & Kumar C, *J Opt Commun*, (2020).